Theory of binary alloys including short-range order properties

L. M. Falicov and Felix Yndurain*
Department of Physics,† University of California, Berkeley, California 94720
(Received 23 June 1975)

A new method for studying the electronic structure of binary alloys within the tight-binding framework is presented and developed in detail. The method involves treating part of the system exactly as a cluster of atoms and simulating the rest of the environment by connecting to each atom at the surface of the cluster a Bethe lattice of the same coordination number. The method includes from its inception the idea of short-range correlation effects of a nearest-neighbor order parameter. Clusters of different size have been studied and analyzed in detail. An illustrative example is presented to show the *striking differences* which appear in various concentration sequences. These sequences are selected to be (i) random, (ii) with a tendency to segregation, and (iii) with a tendency to form binary compounds. The results emphasize the need to include short-range correlation effects when dealing with alloys. The method also provides a clear identification of localized states. In addition, it gives very naturally the position of band edges and energy gaps. The method, when averaged over all alloys with equal concentration and all short-range order parameters, reproduces in a satisfactory way the results of the single-site coherent-potential approximation.

I. INTRODUCTION

In the last ten years there has been an increasing interest in both the experimental and theoretical study of the electronic properties of binary alloys and disordered system.[1-3] Most of the theoretical work has been confined to the completely disordered cases in spite of the fact that a large number of experiments show the importance of the local environment on the magnetic and electronic properties of alloys.[4] Among the various theoretical approaches, the most common by far has been the single-site coherent-potential approximation[5] (CPA). This approximation considers only the fluctuations of the site atomic energy levels, which are supposed to depend only on the chemical nature of the atom occupying that site. The CPA, then, cannot take proper account of local environment effects like short-range order. There have been several extensions of CPA to include correlation between the different sites,[6-11] the main shortcomings of these extensions being that they are either too formal to be of any value in practical applications[6] or they give several possible solutions and the choice of the right one is not unambiguous.[7,8] In addition, some of the proposed approximations lead to unphysical results, such as negative densities of states.[9-11]

Another approach to the study of the electronic properties of binary alloys has been to incorporate the local order in a Green's-function formalism.[12] This approximation is quite interesting, but so far it gives only partial results. In addition to the already mentioned drawbacks, it should be pointed out that none of the above approximations as they stand can take into account topological disorder because they use the $\vec{k}$-space representation to get the density of states.

In this paper, we study the electronic properties of a binary alloy using a method recently developed by the authors[13] which has the following characteristics: (a) It incorporates the short-range order of the alloy in a very natural way; (b) It deals with real potentials instead of "mean" or "effective" ones, albeit only in the tight-binding approximation; and (c) It takes proper account of both topological and substitutional disorder.

We assume that we are dealing with a binary alloy of constituents A and B with concentrations x_A and x_B, respectively ($x_A + x_B = 1$), in such a way that each atom is surrounded by z nearest-neighbor atoms throughout the whole system. We use in this case the following tight-binding Hamiltonian:

$$H = \sum_i U_i \, |i\rangle\langle i| + \sum_{<ij>} V_{ij} \, |i\rangle\langle j| \,, \tag{1.1}$$

where $|i\rangle$ is the atomic orbital wave function of the site i. U_i takes the values U_A and U_B depending on whether the i atom is of class A or B. The summation $\langle ij\rangle$ is restricted to nearest neighbors only. V_{ij} takes the values V_{AA}, V_{BB}, or V_{BA} depending on whether the ith and jth atoms—that is, the (i,j) bond—are both of class A, both of class B, or one of each class.

In addition to the concentrations x_A and x_B, we characterize the alloy by the short-range-order parameters p_A and p_B.[13] The parameter p_A (p_B) gives the probability that when choosing a nearest-neighbor pair such that one of the atoms is of class A (B), the other atom is of the same class. In this way, we define the parameters λ_A (λ_B) and q_A (q_B) by

$$\lambda_A \equiv p_A - q_A \equiv 2p_A - 1 \tag{1.2}$$

(and similarly for λ_B) such that $\lambda_A = 1$ corresponds to a complete segregation—all atoms of class A surrounded by atoms of class A—and $\lambda_A = -1$ corresponds to a perfect binary compound—all atoms of class A surrounded by atoms of class B. The parameter q_A (q_B) defined in (1.2) gives the probability that when choosing a nearest-neighbor pair such that when one of the atoms is of class A (B), the other atom is of class B (A). Of course, the allowed values of q_A and q_B are limited by the concentration x_A and by the requirement of conservation of the total number of particles. If use is made of the definition of q_A and q_B, when we count the number of pairs of nearest neighbors in the system formed by two different atoms, we get

$$x_A q_A \equiv x_B q_B \tag{1.3}$$

or, equivalently,

$$x_A \lambda_A - x_B \lambda_B \equiv x_A - x_B \,. \tag{1.4}$$

With the above mentioned characteristics of the alloy in hand, we calculated the local density of states around the atoms in an alloy using the cluster–Bethe-lattice method.[13,14] In this paper we are concerned mostly with diagonal disorder only, i.e., $V_{AA} = V_{AB} = V_{BB}$; the results for the off-diagonal disorder will be reported in a future publication.

The remainder of this paper is organized as follows: In Sec. II we extend the cluster–Bethe-lattice method to study binary alloys; the formalism is presented and described in detail. In Sec. III we study the simplest possible cluster, namely, one-atom and $(1+z)$-atom clusters. Although they are very simple, they give an enormous amount of information. We define three different sequences: random, segregation, and binary compound. In the case of the simple clusters we calculate exactly the density of states for these sequences. We find, as expected, completely different results for different cases. In addition, distinction between localized and extended states is made and discussed in detail. In Sec. IV we study, for $z = 4$, clusters of 17 and 29 atoms. We generate a *random* distribution of clusters and, in addition to analyzing each of them, we calculate the *averaged* density of states which compares satisfactorily with CPA calculations. Finally, in Sec. V, some concluding remarks are made.

II. EXTENSION OF CLUSTER-BETHE-LATTICE METHOD TO STUDY OF BINARY ALLOYS

Given a binary alloy characterized by the concentrations x_A and x_B of constituents A and B, respectively, and by the short-range parameters p_A and p_B, we seek a method to determine the local density of electronic states about particular atoms. We therefore select a given atom called 0 of, say, class A. We take a representative cluster of $1+n$ atoms which includes the central atom, and saturate the "dangling" bonds of the atoms in the periphery of the cluster by the appropriate Bethe lattices. We are aiming at the use of standard procedures[14] for the calculation of the density of states at atom 0.

It is evident that in order to obtain a meaningful final result the selection of the central atom, the cluster, and the Bethe lattices must be made carefully.

In order to illustrate our procedure, we chose the 1+4 cluster of Fig. 1 corresponding to an atom and its four nearest neighbors for an alloy of coordination number $z = 4$. We label such a cluster C.

If atoms 0, 1, and 2 are of class A, and 3 and 4 of class B, the use of Dyson's equation

$$EG = 1 + HG \,, \tag{2.1}$$

where G is the Green's function and H the Hamiltonian (1.1), yields a set of equations[14]

$$\begin{aligned}
(E - U_A)\langle 0|G|0\rangle &= 1 + V_{AA}\langle 1|G|0\rangle + V_{AA}\langle 2|G|0\rangle \\
&\quad + V_{AB}\langle 3|G|0\rangle + V_{AB}\langle 4|G|0\rangle \,, \\
(E - U_A)\langle 1|G|0\rangle &= V_{AA}\langle 0|G|0\rangle + 3\bar{V}_A T_A \langle 1|G|0\rangle \,, \\
(E - U_A)\langle 2|G|0\rangle &= V_{AA}\langle 0|G|0\rangle + 3\bar{V}_A T_A \langle 2|G|0\rangle \,, \\
(E - U_B)\langle 3|G|0\rangle &= V_{AB}\langle 0|G|0\rangle + 3\bar{V}_B T_B \langle 3|G|0\rangle \,, \\
(E - U_B)\langle 4|G|0\rangle &= V_{AB}\langle 0|G|0\rangle + 3\bar{V}_B T_B \langle 4|G|0\rangle \,.
\end{aligned} \tag{2.2}$$

In (2.2), $\bar{V}_A$ and $\bar{V}_B$ are effective potentials for the Bethe lattice and T_A and T_B are the transfer matrices, both of which characterize the connection of atoms A and B to their respective Bethe lattices. If $\bar{V}_A$, $\bar{V}_B$, T_A, and T_B are known, solution of (2.2) to obtain $\langle 0|G|0\rangle$ is straightforward. From $\langle 0|G|0\rangle$ we obtain

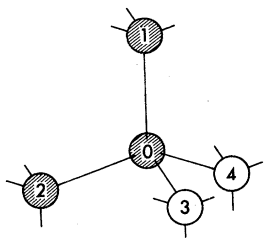

FIG. 1. Five-atom cluster formed by the central atom labeled 0 and its four nearest neighbors. The shaded atoms correspond to atoms of class A; the unshaded atoms correspond to atoms of class B. Each of the noncentral atoms has its three dangling bonds connected to a Bethe lattice of coordination number $z = 4$.

$$n_0(E, C) = -\pi^{-1}\,\mathrm{Im}\langle 0|G|0\rangle\,, \tag{2.3}$$

where $n_0(E, C)$ is the local density of states of atom 0 of cluster C. The total density of states is then given by

$$n(E) = \sum_C \omega_C n_0(E, C)\,, \tag{2.4}$$

where all possible clusters C contribute, each with its proper weight ω_C.

The problem therefore consists of four parts: (a) Determination of the transfer matrices T_A and T_B and the effective potentials $\bar{V}_A$ and $\bar{V}_B$; (b) Selection of the proper clusters and their attendant weights ω_C; (c) Solution of the various systems of equations, similar to (2.2); and (d) Proper averaging, according to (2.4).

We first focus our attention on (b). It is evident that clusters with central atom A contribute, relative to clusters with central atom B, in a ratio proportional to the concentrations x_A/x_B. For each given central atom, say, A, the weight of the various clusters should be compatible with the short-range-order parameter p_A. The calculation of the weights becomes more involved as the size of the cluster increases. In the 1+4 example of our illustration, with short-range-order parameters p_A and p_B, the weights are

$$\begin{aligned}
&A:AAAA, && \omega = x_A p_A^4\,,\\
&A:AAAB, && \omega = 4x_A p_A^3 q_A\,,\\
&A:AABB, && \omega = 6x_A p_A^2 q_A^2\,,\\
&A:ABBB, && \omega = 4x_A p_A q_A^3\,,\\
&A:BBBB, && \omega = x_A q_A^4\,,\\
&B:BBBB, && \omega = x_B p_B^4\,,\\
&B:BBBA, && \omega = 4x_B p_B^3 q_B\,,\\
&B:BBAA, && \omega = 6x_B p_B^2 q_B^2\,,\\
&B:BAAA, && \omega = 4x_B p_B q_B^3\,,\\
&B:AAAA, && \omega = x_B q_B^4\,.
\end{aligned} \tag{2.5}$$

For larger clusters it may become more expedient to resort to a random sampling of clusters compatible with the above conditions.

To determine a good expression for the effective potentials $\bar{V}_A$ and $\bar{V}_B$ and the matrices T_A and T_B, we first choose to measure our energies from the average value of U_A and U_B, i.e.,

$$U_A + U_B = 0, \quad U_A = U, \quad U_B = -U\,, \tag{2.6}$$

and focus our attention on V_A and T_A only (V_B and T_B are obtained by changing $U \to -U$, $p_A \to p_B$, and $V_{AA} \to V_{BB}$). In the two limiting cases $p_A = 1$ and $p_A = 0$, the transfer matrices are well known. In the first case, T_A is the solution of[14]

$$\begin{aligned}
&(E-U)T_A = V_{AA} + (z-1)V_{AA}T_A T_A'\,,\\
&(E-U)T_A' = V_{AA} + (z-1)V_{AA}T_A' T_A\,,
\end{aligned} \qquad p_A = \lambda_A = 1\,, \tag{2.7}$$

which gives the solution

$$T_A(E, 1) = T_A'(E, 1) = [\,2(z-1)V_{AA}]^{-1} \times\{(E-U) \pm [\,(E-U)^2 - 4(z-1)V_{AA}^2]^{1/2}\}\,. \tag{2.8}$$

In the case of the binary compound $p_A = 0$ and $\lambda_A = -1$, T_A is the solution of[15]

$$\begin{aligned}
&(E-U)T_A' = V_{AB} + (z-1)V_{AB}T_A T_A'\,,\\
&(E+U)T_A = V_{AB} + (z-1)V_{AB}T_A T_A'\,,
\end{aligned} \qquad \lambda_A = -1\,, \tag{2.9}$$

which yields

$$T_A(E, -1) = [\,2(z-1)V_{AB}]^{-1} \times\left[(E-U) \pm \left((E-U)^2 - \frac{4(z-1)V_{AB}^2(E-U)}{E+U}\right)^{1/2}\right]\,, \tag{2.10}$$

$$T_A'(E, -1) = [\,2(z-1)V_{AB}]^{-1} \times\left[(E+U) \pm \left((E+U)^2 - \frac{4(z-1)V_{AB}^2(E+U)}{E-U}\right)^{1/2}\right]\,.$$

For a completely random environment, i.e., for an atom A surrounded with equal probability by A or B atoms ($p_A = 0.5$, $\lambda_A = 0$), we take for the transfer matrix and the connecting potential a virtual crystal approximation,[16] i.e., we replace

$$\overline{V}_A = \tfrac{1}{2}(V_{AA} + V_{BB}), \quad \overline{U} = \tfrac{1}{2}(U_A + U_B) = 0,$$

which yields

$$T_A(E, 0) = T'_A(E, 0) = [2(z-1)\overline{V}_A]^{-1}\{E \pm [E^2 - 4(z-1)\overline{V}_A^2]^{1/2}\}. \tag{2.11}$$

Given the three values $\lambda_A = 1$, $\lambda_A = 0$, and $\lambda_A = -1$, we now introduce *ad hoc* interpolation formulas, which yield the correct results in those three cases:

$$\overline{V}_A(\lambda_A) = \tfrac{1}{2}[(1+\lambda_A)V_{AA} + (1-\lambda_A)V_{AB}], \tag{2.12}$$

$$T'_A(E, \lambda_A) = [2(z-1)\overline{V}_A]^{-1}\left[(E - \lambda_A U) \pm \left((E-\lambda_A U)^2 - \frac{4(z-1)\overline{V}_A(E-\lambda_A U)}{E - |\lambda_A| U}\right)^{1/2}\right], \tag{2.13}$$

and

$$T_A(E, \lambda_A) = [2(z-1)\overline{V}_A]^{-1}\left[(E - |\lambda_A| U) \pm \left((E-|\lambda_A| U)^2 - \frac{4(z-1)\overline{V}_A(E-|\lambda_A| U)}{E - \lambda_A U}\right)^{1/2}\right]. \tag{2.14}$$

These three formulas constitute only an interpolation scheme, which has several appealing features and physically meaningful properties: (a) It replaces the actual random solid by one in which the interactions related to an atom A are given by the weighted average (2.12), and $\overline{V}_A$ depends crucially on the short-range parameter λ_A. (b) It effectively replaces a nearest neighbor to A by an atom with an effective intra-atomic potential $\lambda_A U$, and the second nearest neighbors have an effective potential $\lambda_A^2 U$, etc. (c) It satisfies *post hoc* the necessary (although by no means sufficient) condition that, when substituted into the proper Green's functions (2.2), the imaginary part of $\langle 0|G|0\rangle$, integrated over all values of E, yields the required value of 1.

This interpolation procedure completes the scheme to calculate the density of states (2.4). The short-range properties of the alloy are both included in the cluster—through the weights ω_C—and in the Bethe lattice. The latter provides an appropriate boundary condition for the former and makes calculations with small clusters, even as small as a single atom, meaningful. It also provides an infinite system where the electronic wave functions may propagate, and therefore a natural framework where the problem of localized versus extended states may be discussed.

III. STUDY OF CLUSTERS OF 1 AND 5 ATOMS

In this section we apply the method of Sec. II to study in detail the density of states corresponding to a single atom surrounded by the Bethe lattice and also the density of states corresponding to a cluster of $1+z$ atoms connected to the Bethe lattice. These two examples can be calculated exactly, and although they seem oversimplified pictures of an alloy, they give an enormous amount of information that helps us to understand more complicated cases. In the rest of the paper we are going to assume that $z = 4$ and that there is no off-diagonal disorder, i.e., $V_{AA} \equiv V_{AB} \equiv V_{BB} = V$. In addition, $U = 2.5V$ in our examples.

A. One-atom cluster

Let us take one atom of, say, class A surrounded by the Bethe lattice of coordination number 4. The diagonal part of the Green's function is the atom is given by

$$\langle 0|G|0\rangle = [E - U - 4VT_A(E, \lambda_A)]^{-1}. \tag{3.1}$$

The local density of states is given by (2.3).

When we study the imaginary part of the diagonal matrix element of the Green's function (3.1) we notice that there are two different contributions to the density of states. One contribution depends on the sign of the expression inside the square root in T_A (2.14); for values of E such that

$$(E - U\lambda_A)^2 - \frac{4(z-1)V^2(E - U\lambda_A)}{(E - U|\lambda_A|)} \tag{3.2}$$

is negative, the transfer matrix T_A is complex with a nonvanishing imaginary part, and thus the local density of states is also nonvanishing. Another contribution is given by the poles of $\langle 0|G|0\rangle$. When the diagonal matrix element of the Green's function has a pole, the density of states is a δ function. Of course, when the δ function appears at energies such that (3.2) is positive, the two contributions to the density of states never overlap. The contribution at energies such that (3.2) is negative is continuous, whereas the δ-function contribution gives a set of discrete levels.

The values of E such that (3.2) is equal to zero correspond to the edges of the continuous bands. The position of these band edges depends very sensitively on the value of λ_A. In Table I we have listed the positions of the band edges for a complete range of values of λ_A; in Fig. 2, we have plotted the corresponding local density of states. In addition, in Table I we also include the weight (residue of the pole of $\langle 0|G|0\rangle$) of the δ function

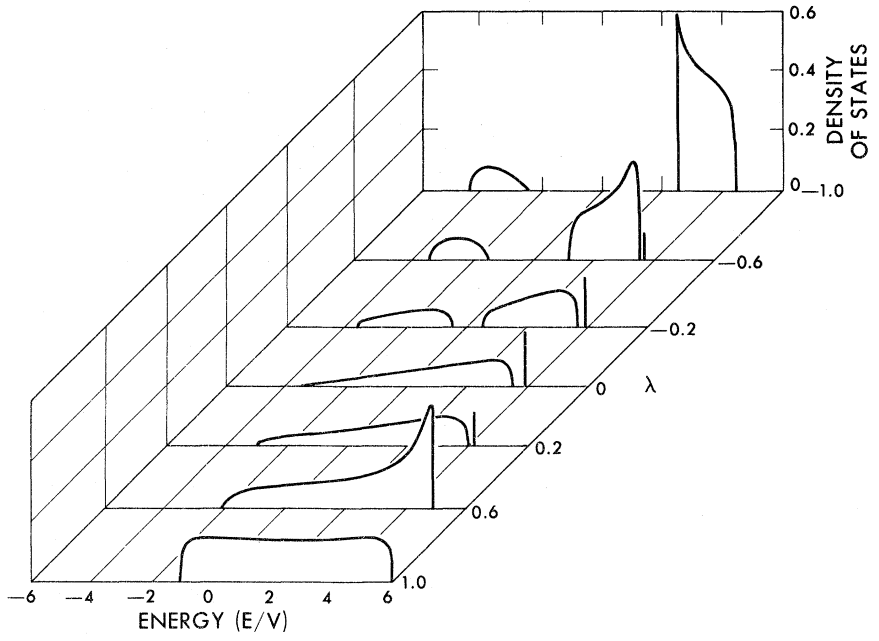

FIG. 2. Local density of states for a single A-atom cluster as a function of the short-range-order parameter λ ($U=2.50V$). The energy is in units of the hopping integral V.

for the same values of λ_A. There is a maximum of one δ function because there is only one state in the cluster (A atom). Since the transfer matrix $T_A(E, \lambda_A)$ transfers from the atom A to the rest of the infinite Bethe lattice, the states due to a nonvanishing imaginary part on $T_A(E, \lambda_A)$ are delocalized states, extending throughout the whole system. On the other hand, the δ-function states are no longer present far away from the central atom. They are localized around the cluster (one atom, in this case) and decay exponentially into the Bethe lattice. This localization is related to the probability that the central atom A is surrounded by B atoms giving rise to a localized state.

With this simple model, one atom connected to the Bethe lattice, we can make a very clear distinction between localized and delocalized states; the Bethe lattice, of course, provides the band-edge positions independently of the size of the cluster. The above discussion is therefore valid for any cluster. Looking at Fig. 2 and Table I, we realize that there is a gap between extended states when $\lambda_A < 0$. This is due to the fact that when $\lambda_A < 0$ there is a tendency to form a binary compound and a gap opens in the middle of the band (of course, the gap is maximum when $\lambda_A = -1$). This result is confirmed when dealing with bigger clusters (see Sec. IV).

Looking at the density of states when we go from $\lambda_A = 1$ to $\lambda_A = -1$ (Fig. 2 and Table I), we see how the localized state splits off the continuous band. When $\lambda_A = 0.6$, there is a sharp peak in the density of states close to the band, and when $\lambda_A = 0.2$, a state has already separated from the band. The weight of the δ function gives the total weight at the central atom of the charge density of the isolated state. In particular, when $\lambda_A = 0$, the separation in energy between the position of the δ function and the band edge as well as the weight of the δ function are maxima. This is so because when $\lambda_A = 0$ there is no correlation between atoms of class A and class B in the Bethe lattice, giving rise to the most favorable situation to get localized states.

It can be easily seen that, in order to get a δ function, λ_A has to be such that

TABLE I. Characteristics of the density of states for a single A-atom cluster as a function of the short-range-order parameter λ_A($U=2.5V$ throughout).

λ	Position of δ function	Weight	Band edges
1.0			$5.964V$, $-0.964V$
0.8			$5.464V$, $-1.464V$
0.6			$4.964V$, $-1.964V$
0.4	$4.500V$	0.060	$4.714V$, $-2.214V$
0.2	$4.181V$	0.434	$3.964V$, $-2.964V$
0.0	$3.903V$	0.562	$3.464V$, $-3.464V$
−0.2	$3.819V$	0.548	$\pm 3.500V$, $\pm 0.500V$
−0.4	$3.778V$	0.481	$\pm 3.606V$, $\pm 1.000V$
−0.6	$3.811V$	0.280	$\pm 3.775V$, $\pm 1.500V$
−0.8			$\pm 4.000V$, $\pm 2.000V$
−1.0			$\pm 4.272V$, $\pm 2.500V$

$$(1/U)\{U-[(z-2)/(z-1)^{1/2}]V\} \geq \lambda_A \geq \tfrac{1}{2}[-z+(z-2)(1+4V^2/U^2)^{1/2}]\,. \tag{3.3}$$

It is also interesting to notice that for this simplest cluster we cannot have localized states inside the gap. The reason is that the energy of the localized state should be such that $|E_L|>U$. The band-gap edges, on the other hand, appear only through the A-B interaction, and are always located at values $|E_{\text{band edge}}|\leq U$.

Let us finish this discussion of the atom–Bethe-lattice system by pointing out that in order to get a localized state at all, U has to be larger than a critical value U^C,

$$U^C = V(z-2)/(z-1)^{1/2}\,. \tag{3.4}$$

This value is obtained from (3.3) when $\lambda_A = 0$.

B. Five-atom cluster

So far we have characterized the alloy by means of the parameters λ_A and λ_B only. We have said nothing about the concentration. It is clear that the range of the allowed values of λ_A and λ_B is constrained by the concentration. The sum rule (1.4) must be satisfied. In addition, since both λ_A and λ_B can vary only between -1 and $+1$, we obtain the extra condition that

$$1-2x_B/x_A \leq \lambda_A \leq 1 \quad \text{for } x_A > x_B\,. \tag{3.5}$$

The limiting case $\lambda_A = 1$ corresponds to the case when all the A and B atoms tend to be completely spatially segregated. The limit $\lambda_A = 1-2x_B/x_A$ corresponds to the case when *all* the B atoms tend to form a perfect binary compound with a *fraction* of the A atoms. The rest of the A atoms (proportional to $x_A - x_B$) are located at random.

We then may define sequences of alloys[13] such that as x_A varies from 0 to 1, λ_A takes a well-defined series of values. In this way, we write the following:

Segregation sequence. All the atoms of class A (B) are surrounded by atoms of class A (B). The alloy has a tendency to segregate into two separate regions, the A and B regions, respectively. For this sequence, we get

$$\lambda_A = \lambda_B = 1 \quad \text{for any } x_A\,. \tag{3.6}$$

Random sequence. In this sequence, there is no short-range correlation between the atoms. This sequence corresponds in some respect to the philosophy of the virtual-crystal[16] or coherent-potential[5] approximations. In this sequence, we have

$$\lambda_A = x_A - x_B \quad \text{and} \quad \lambda_B = x_B - x_A\,. \tag{3.7}$$

Binary-coumpound sequence. All the atoms of class A want to be surrounded by atoms of class B and vice versa. If the concentration is not $x_A = x_B = 0.5$, only the minority class can form a perfect binary compound. In accordance with (3.5), we get

$$\lambda_A = -1;\quad \lambda_B = 1-2x_A/x_B \quad \text{if } x_A \leq x_B\,,$$
$$\lambda_B = -1;\quad \lambda_A = 1-2x_B/x_A \quad \text{if } x_A \geq x_B\,. \tag{3.8}$$

In order to study these three sequences in detail, we have chosen a cluster of five atoms, the central atom and its four nearest neighbors. We can study all possible clusters (*AAAAA*, *AAAAB*, *AAABB*, *AABBB*, *ABBBB*, and *BBBBB*). Each cluster is weighted consistently with a binomial distribution compatible with λ_A and λ_B, i.e., the values (2.5). The local density at the central atom in each cluster contributes to the total density of states in an amount proportional to its concentration.

In Fig. 3 we show the density of states corresponding to the five-atom cluster for the three above-mentioned sequences and for different concentrations. We show the total density of states by analyzing the central atom in each of the ten clusters given by (2.5).

For the values here chosen ($V=1$, $U=2.5V$), the segregation sequence shows a single wide band extending from the bottom of the band B to the top of band A, with a considerable incoherent overlap in the middle. The hump in the distribution becomes more pronounced at the equal concentration $x_A = x_B = 0.5$. For this sequence there are neither localized states nor energy gaps. For larger values of U ($U > [4(z-1)V^2]^{1/2}$) an "atomic" gap appears throughout the whole range of concentrations, $0 \leq x_A \leq 1$.

The random sequence shows completely different behavior. Localized states appear in the middle range of concentrations, $0.23 < x_A < 0.77$. There is no energy gap in the middle, but a sizeable depression in the density of states is apparent, mostly for $x_A \approx 0.5$. In the middle range of concentrations no energy gap is present, regardless of the values of the parameters U and V.

The binary-compound sequence exhibits a minority-component-induced gap throughout most of the concentration range. In our particular example, the gap is of "ionic" character near the middle, $0.33 < x_A < 0.67$ [where, according to (3.8), both λ_A and λ_B are negative], and mixed ionic-atomic gap close to the end of the concentration range, $x_A < 0.23$ and $x_A > 0.77$, where the band edge of the single band lies inside the ionic gap. In this last

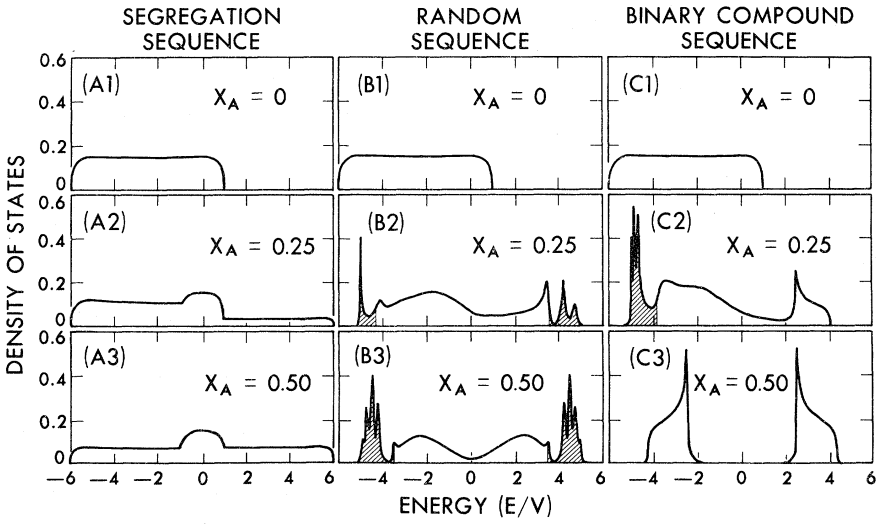

FIG. 3. Total density of states for the five-atom cluster. Three sequences are shown—(A) segregation sequence, (B) random sequence, and (C) binary compound—for three concentrations: (1) $x_A=0$, $x_B=1$; (2) $x_A=0.25$, $x_B=0.75$; and (3) $x_A=x_B=0.50$. The two additional concentrations (4) $x_A=0.75$, $x_B=0.25$ and (5) $x_A=1$, $x_B=0$ can be obtained from (2) and (1), respectively, by changing the sign in the energy axis. Shaded areas correspond to states localized in the cluster. A very small constant imaginary part has been added to the energies to make the density of states due to localized states visible in the plots. The energy is in units of the hopping integral V.

case, there is an incoherent superposition of states which are itinerant and extend either mostly throughout the majority-species atoms or coherently through the binary-compound portion of the alloy. The ionic gap is, of course, maximum for $x_A=x_B=0.5$, which is the perfect binary compound. Localized states appear for concentrations not in the end or middle ranges; they are, in general, localized about the majority species atoms.

Since the band gaps and positon of the band edges are a function of the boundary conditions (Bethe-lattice) exclusively, the above results are quite general and do not depend on the size of the cluster. The effect of the cluster size appears only on the structure and on fine details of the density-of-state function.

IV. STUDY OF CLUSTERS OF DIFFERENT SIZE: COMPARISON WITH CPA

In order to study how the density of states converges towards the exact result, we have studied the density of states corresponding to clusters of 17 and 29 atoms in the topological arrangement of the diamond lattice. The cluster of 29 atoms is drawn in Fig. 4; the cluster of 17 atoms can be obtained from it by removing all the atoms beyond the 16th (see Fig. 4). The 17-atom cluster contains the first- and second-nearest neighbors of the central atom. The 29-atom cluster contains in addition the third-nearest neighbors in such a way that 12 sixfold rings of bonds passing through the central atom are taken into account. Topological properties of the lattice are therefore introduced at this point. For clusters with a number of atoms larger than the small ones considered in Sec. III, the combinational aspects of calculating

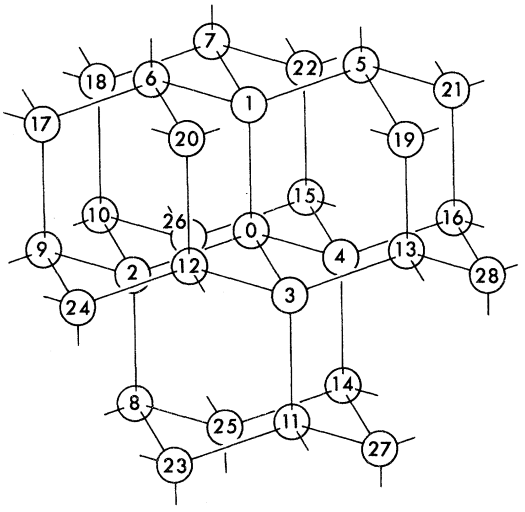

FIG. 4. Position of the atoms in the cluster of 1+28 atoms in the diamond structure arrangement. The central or reference atom is labeled 0. Bethe lattices of coordination number 4 are connected to the dangling bond of atoms labeled 5–16 and to the two dangling bonds of atoms labeled 17–28.

the weights ω_C as well as the sheer number of different clusters to consider makes the calculation extremely impractical. We resort therefore to a random selection of a not-too-large number of clusters (78 in our case) to make the computation manageable. The clusters which we consider are chosen at random from a sampling of the $x_A = x_B = 0.5$ concentration only. In this case, (1.4) requires $\lambda_A = \lambda_B = \lambda$. Each of these random clusters was assumed to correspond to that λ which is obtained by the nearest-neighbor pair analysis of the cluster (40 pairs in the case of a cluster of 29 atoms).

For the clusters of 29 atoms, the random selection was made with ν atoms of class A and $28 - \nu$ atoms of class B with weights proportional to a binomial distribution

$$W(\nu) = 28!/\nu!(28-\nu)! \ .$$

The central atom was alternately considered to be of classes A and B. We took 2×78 clusters in this form, of which 14 had a central atom A and an equal number $(14+14)$ of A and B atoms surrounding it, and another 14 had a central atom B with exactly the same distribution of the 28 noncentral atoms of the cluster. Analysis of the 40 nearest-neighbor pairs of the 156 clusters yielded a variety of λ values. The histogram of Fig. 5 shows the λ distribution of our clusters. We see that the histogram does not differ radically from a Gaussian curve to which it must converge when the number of clusters becomes infinitely large.

The random distribution for the clusters of 17 atoms was obtained by removing the atoms beyond

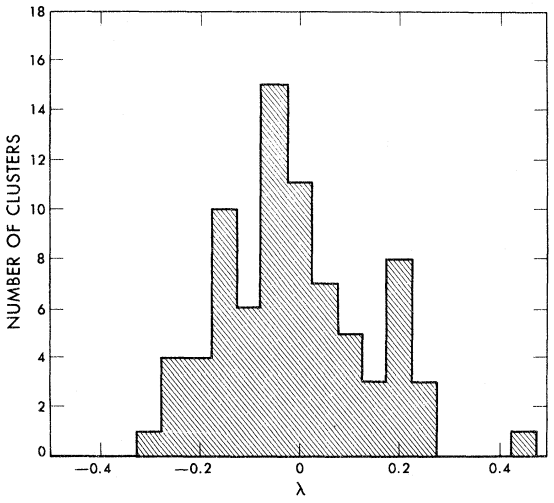

FIG. 5. Number of clusters with the same λ corresponding to our random sampling. Only the 78 clusters with central A atoms are reported.

the 16th (see Fig. 4) of the 29-atom clusters described above. For the clusters of 17 atoms, we took the same λ as the corresponding 29-atom cluster from which it originated. In Figs. 6–8 we have plotted the density of states corresponding to three particular clusters of our distribution. We have plotted the density of states of a cluster of 29 atoms and its corresponding clusters of 17 and 5 atoms. Since we take the same λ for the three different clusters (5, 17, and 29 atoms), the range of energies where the states are localized is independent of the size of the cluster.

The positions of the atoms in the three clusters corresponding to Figs. 6–8 are given in Table II. It should be noticed that in the cluster of Fig. 6 the central atom of class A is surrounded by three atoms of class A and one of class B. In the cluster of Fig. 7 the central atom has two A atoms and two B atoms as nearest neighbors. In the cluster of Fig. 8 the central atom has three B atoms and one A atom as nearest neighbors. The direct comparison of (a)–(c) in Figs. 6–8 shows that the local configuration determines the over-all shape of the density of states. The main difference in the density of states is in the number and energy of the localized states; i.e., δ functions. The number of such localized states cannot exceed the number of atoms in the cluster; hence the larger the size of the cluster, the more δ-function singularities are likely to appear. It is, however, important to remark that the total weight of the density of localized states projected onto the central atom is insensitive to the size of the cluster, and that the over-all energy range—and hence the degree of localization—of the localized states does not vary appreciably with the size of the cluster.

Since we compute total density of states according to (2.4) by adding local densities of states, it is obvious from the observations above that very small clusters—even the simplest cluster of one atom—yield a fairly good description of the total density of localized states.

Although the total density of states of the five-atom cluster looks different to the corresponding ones of 17 or 29 atoms, the gross features remain throughout. Figure 6 shows itinerant states which exhibit a peak and a shoulder for a five-atom cluster and a double-peak structure for the corresponding 17- and 29-atom clusters. The high-energy shoulder of Fig. 6(a) gets enhanced by, and combined with, the localized δ functions arising from the larger clusters.

Figure 8, on the other hand, shows a simple one-peak structure in the itinerant states of the five-atom cluster which splits and separates into two peaks for larger clusters. The high-energy peaks merge smoothly into the multiply-structured local-

ized states.

In Fig. 7, the five-atom cluster yields for the itinerant states a very similar structure to those of the larger clusters.

Several additional features are worth remarking upon. It is possible for large clusters to produce localized states in the ionic (negative λ) gap [see Figs. 7(b) and 7(c) and 8(b) and 8(c)]. Also, in contrapositon with perfectly ordered solids,[14,15] the presence of rings of bonds in an alloy produces little or no effect in the density of states. This can be clearly seen by comparing Figs. 6(b), 7(b), and 8(b)—corresponding to 17-atom clusters and no rings—with Figs. 6(c), 7(c), and 8(c)—which correspond to 29-atom clusters and 12 sixfold rings. The only apparent effect of the closed rings seems to be to extend slightly away from the itinerant band the "band" of localized states, i.e., to produce localized states which are more localized in the cluster.

In order to test the general validity of our theory we have compared our results with the results obtained with the CPA.[5] In the CPA, it is assumed that there is no correlation between the atoms in the alloy and thus the density of states is a function only of the concentration and chemical composition.

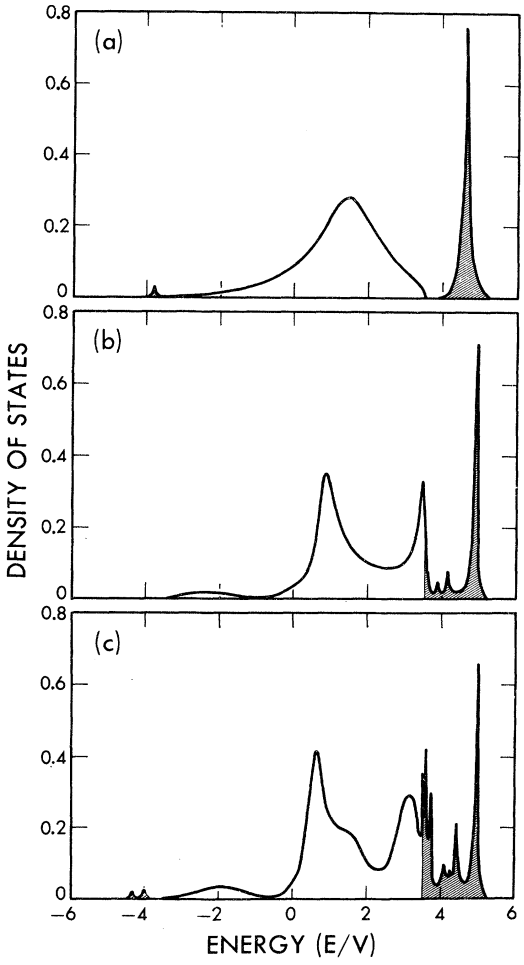

FIG. 6. Local density of states corresponding to the cluster 1 of Table II. (a) Local density of states corresponding to the five-atom cluster. We obtain this cluster by taking only atoms 0–4 of cluster 1 described in Table II. (b) Local density of states corresponding to the 17-atom cluster. We obtain this cluster by taking only the atoms 0–16 of cluster 1 described in Table II. (c) Local density of states corresponding to the 29-atom cluster 1 of Table II. Shaded areas correspond to states localized in the cluster. A very small constant imaginary part has been added to the energy to make the density of localized states visible in the plots. In this case, $\lambda=0$ and $U=2.50V$. The energy is in units of the hopping integral V.

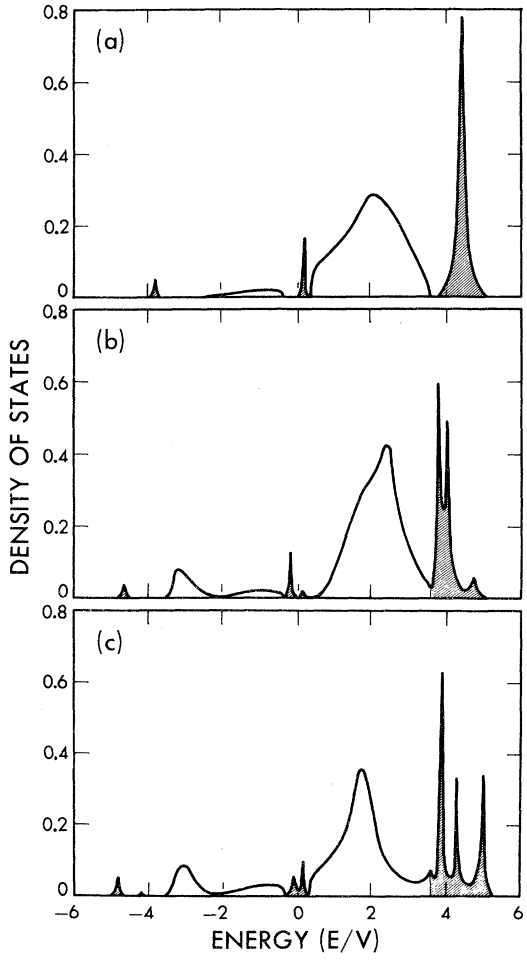

FIG. 7. Same as for Fig. 6, for cluster 2 of Table II and $\lambda=-0.15$.

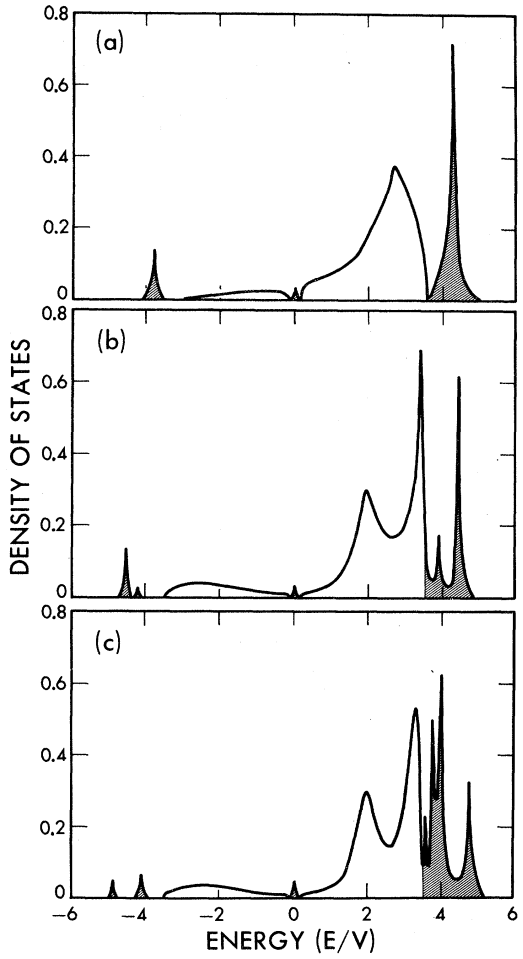

FIG. 8. Same as for Fig. 6, for cluster 3 of Table II and $\lambda = -0.05$.

We have calculated the averaged density of states of the 156-cluster distribution, and have done this for the clusters of 17 and 29 atoms. In Fig. 9 the average total density of the clusters of both 17 and 29 atoms are drawn. In addition, the exact density of states for the Bethe lattice within the CPA is also shown. As we can see, our density of states compares satisfactorily with the CPA. Of course, we get a structure that does not appear in the CPA; this is in part due to our random sampling, and to the fact that we have a finite number of δ functions. The position of the band edges is very similar; where the CPA shows a gap, we get a pronounced dip in the density of states. In Fig. 9(b) we have plotted the average total density of states corresponding to the 29-atom cluster. Again, we notice here that the density of states does not change much when we increase the number of atoms in the cluster. We conclude that the density of states drawn in Fig. 9(b) corresponds to our particular random distribution, and that the structure found in the density of states is real and does not depend on the method of calculation.

The above average (Fig. 9) corresponds to a random alloy with no short-range correlations; for this case our method does not present very important advantages with respect to previous theories (CPA). Where our method is an improvement over other previous theories is when the alloy is such that short-range correlation exists. Suppose, for instance, that the alloy in which we are interested is such that $\lambda_A = -0.15$. In order to calculate the local density of states at an A site, we take the averaged density of states of the clusters in our random sampling with a central atom A and with *the same* λ (-0.15). The averaged density of states for clusters of 17 and 29 atoms are drawn in Fig.

TABLE II. Three random clusters of 29 atoms. Topology corresponds to that of Fig. 4, and the resulting densities of states are shown in Figs. 6–8.

	Cluster 1 (Fig. 6)
Atoms of class A	0, 1, 2, 3, 7, 9, 10, 11, 13, 15, 16, 19, 25, 26, 27
Atoms of class B	4, 5, 6, 8, 12, 14, 17, 18, 20, 21, 22, 23, 24, 28
	Cluster 2 (Fig. 7)
Atoms of class A	0, 1, 2, 9, 10, 11, 12, 13, 17, 18, 19, 21, 24, 25, 26
Atoms of class B	3, 4, 5, 6, 7, 8, 14, 15, 16, 20, 22, 23, 27, 28
	Cluster 3 (Fig. 8)
Atoms of class A	0, 1, 7, 9, 12, 14, 15, 19, 21, 22, 24, 25, 26, 27, 28
Atoms of class B	2, 3, 4, 5, 6, 8, 10, 11, 13, 16, 17, 18, 20, 23

10. In this case, we can again distinguish between localized and extended states. Since $\lambda < 0$, the band of extended states exhibits a gap which is partially filled with localized states. This local (A atom) density of states resembles the by now "classical" picture of a disordered semiconductor[7] with a "mobility gap," i.e., two bands of itinerant states sandwiched between three bands of localized states.

As a last remark, we would like to point out that the appearance of an ionic gap in our calculations when $\lambda < 0$—which is mathematically due to the $|\lambda|$ dependence of our transfer matrices in the interpolation formulas (2.13) and (2.14)—can be *post hoc* confirmed by the results of our calculations. As seen in Fig. 3, a fairly large reduction in the density of states at $E = 0$ appears in the random case; in addition, the over-all averages of Fig. 9, which are heavily dominated by the large clusters, show the pronounced dip in the middle of the band which is due to those clusters which have a large number of unlike pairs, i.e., those clusters with negative λ. We can state categorically that the cluster calculations confirm the qualitative correctness of our calculational scheme.

V. CONCLUSIONS

The technique developed in this paper and the illustrative model and examples presented here have allowed us to introduce a new theory of binary alloys with the following characteristics: (i) It incorporates from the start short-range properties described by a nearest-neighbor order parameter λ. (ii) It can treat in principle any realistic tight-binding model, with an arbitrary number of orbitals per atom and with realistic potential parameters. (iii) It allows for the simultaneous treatment of substitutional and topological disorder. (iv) It produces the expected ionic energy gaps when binary-compound tendencies appear in the random alloy. (v) It gives a natural way of identifying states localized in the cluster[18]; they appear as poles of the Green's function outside of the Bethe-lattice continuum. (vi) Statistical sampling of large clusters and averages across-the-board, regardless of short-range order, reproduce in a satisfactory way the results of the CPA—considered at present the best theory for the single-site, completely disordered alloy.

The technique and the model can of course be improved as well as applied to specific problems. In particular, we can think of the following lines for future research: (a) Application to realistic semiconducting alloys, in particular, germanium-silicon alloys[19] where the available calculations indicate the necessity of including short-range-order considerations in order to explain experimental data. (b) Application of the model to liquid alloys, including those which exhibit as a function of concentration metal-semiconductor transitions.[20] (c) Extension of the theory to second- and higher-neighbor correlations.[21] This in turn should make it possible to treat more general

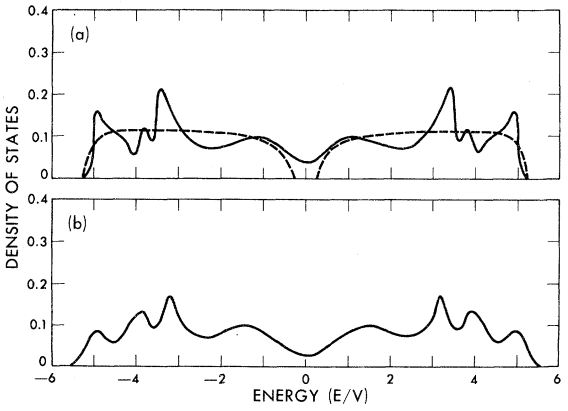

FIG. 9. Total density of states obtained by averaging over the 156 clusters of our random sampling (heavy full lines). (a) Total density of states of the 17-atom cluster (full line) and total density of states given by the coherent-potential approximation (CPA) in the Bethe lattice of coordination number $z = 4$ (broken line). (b) Total density of states of the 29-atom cluster. $U = 2.50V$.

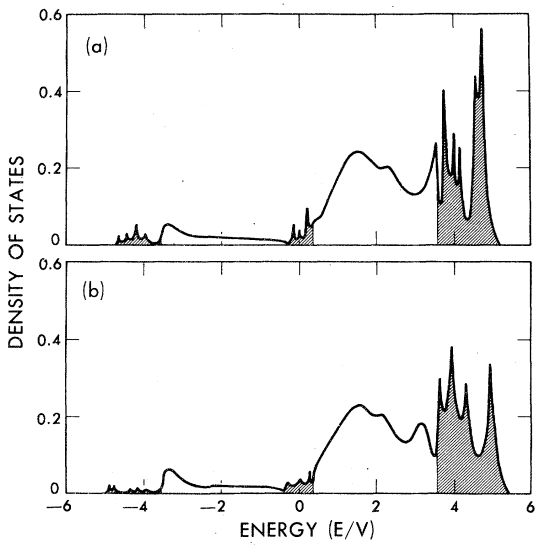

FIG. 10. Averaged local density of states corresponding to the clusters of our random sampling with the central atom of class A and $\lambda = -0.15$. (a) Density of states corresponding to the 17-atom cluster. (b) Density of states corresponding to the 29-atom cluster. Shaded areas correspond to localized states. $U = 2.50V$.

tight-binding Hamiltonians. (d) Improvement of the approximations (2.13) and (2.14) to allow for bonds of varying length, in which case, in addition to topological and substitutional disorders, structural disorder could also be treated by the same approach. (e) A more *ab initio* theory could be attempted to justify or improve the interpolation formulas (2.12)–(2.14) which would give the position of the edges of the bands of delocalized states more precisely. (f) A more extensive theory of localization of electron states[22] could be developed for the model.

We believe, however, that even in its present state, our technique offers new possibilities and paths to investigate the properties of disordered alloys with short-range correlations.

---

*Fulbright fellow under the auspices of the "Program of Cultural Cooperation between the U.S.A. and Spain."

†Work supported in part by the NSF through Grant No. DMR72-03106-A01.

[1]R. J. Elliott, J. A. Krumhansl, and P. L. Leath, Rev. Mod. Phys. 46, 465 (1974).

[2]D. J. Thouless, Phys. Lett. C 13, 93 (1974).

[3]Proceedings of the Michigan State University Summer School on Alloys, edited by W. M. Hartmann, P. A. Schroeder, and C. L. Foiles (Michigan State University, 1972) (unpublished).

[4]See, for instance, B. Mozer, D. T. Keating, and S. C. Moss, Phys. Rev. 175, 868 (1968); J. D. Perrier, B. Tissier, and R. F. Tournier, Phys. Rev. Lett. 24, 313 (1970); J. S. Kouvel and J. B. Comly, *ibid.* 24, 598 (1970).

[5]P. Soven, Phys. Rev. 156, 809 (1967); 178, 9936 (1969); B. Velický, S. Kirkpatrick, and H. Ehrenreich, *ibid.* 175, 747 (1968); S. Kirkpatrick, B. Velický, and H. Ehrenreich, Phys. Rev. B 1, 3250 (1970); L. M. Schwartz and E. Siggia, *ibid.* 5, 383 (1972). See Refs. 1–3 for more information about CPA.

[6]K. F. Freed and M. H. Cohen, Phys. Rev. B 3, 3400 (1971).

[7]F. Brouers, M. Cyrot, and F. Cyrot-Lackman, Phys. Rev. B 7, 4370 (1973).

[8]F. Brouers, F. Ducastelle, F. Gautier, and J. Van der Rest, J. Phys. F 3, 2120 (1973).

[9]W. H. Butler, Phys. Rev. B 8, 4499 (1973).

[10]For a discussion of the application of the Bethe-Peierls approximation to the study of binary alloys (Refs. 7 and 8), see P. N. Sen and F. Yndurain (unpublished).

[11]K. Aoi, Solid State Commun. 14, 929 (1974).

[12]R. G. Woolley and R. D. Mattuck, J. Phys. F 3, 75 (1973).

[13]F. Yndurain and L. M. Falicov, Solid State Commun. (to be published).

[14]J. D. Joannopoulos and F. Yndurain, Phys. Rev. B 10, 5164 (1974).

[15]F. Yndurain and J. D. Joannopoulos, Phys. Rev. B 11, 2957 (1975).

[16]F. Bassani and D. Brust, Phys. Rev. 131, 1524 (1963).

[17]N. F. Mott, *Metal-Insulator Transitions* (Barnes and Noble, New York, 1974), pp. 33 and 44.

[18]S. Kirkpatrick and T. P. Eggarter, Phys. Rev. B 6, 3598 (1972).

[19]D. Stroud and H. Ehrenreich, Phys. Rev. B 2, 3197 (1970).

[20]See, for instance, H. Hoshino, R. W. Schmutzler, and F. Hensel, Phys. Lett. A 51, 7 (1975).

[21]L. M. Schwartz, Phys. Rev. B 7, 4425 (1973).

[22]E. N. Economou and M. H. Cohen, Phys. Rev. B 5, 2931 (1972).